A Dual-Frequency Series-Fed Patch Array Antenna

S. Otto [#*1], A. Rennings [+2], O. Litschke [#3], K. Solbach [*4]

[#] *IMST GmbH*
Carl-Friedrich-Gauß-Straße 2, 47475 Kamp-Lintfort, Germany
[1]otto@imst.de, [3]litschke@imst.de

[*] *Hochfrequenztechnik (HFT) and* [+] *Allgemeine und Theoretische Elektrotechnik (ATE)*
University of Duisburg-Essen, Bismarck-Straße 81, 47057 Duisburg, Germany
[2]andre.rennings@uni-due.de, [4]klaus.solbach@uni-due.de

***Abstract*— A novel dual-frequency concept for series-fed microstrip patch array antennas is proposed. An identical near field distribution following an identical far field characteristic was achieved at two different frequencies. The conventional series fed array comes with a uniform aperture distribution for patches of same width. By exploiting the dispersion of this periodic structure the same cosine aperture distribution at two different frequencies is obtained. Due to the cosine aperture distribution a low side lobe level of 23 dB is intrinsically achieved for the two operating frequencies, 23 GHz and 25 GHz. This concept is particularly suited for small frequency ratios** $(f_+/f_- < 1.3)$**.**

I. Introduction

Microstrip series fed patch array antennas are known for almost 30 years [1] and have also been examined in the context of traveling wave and resonator antennas [2]. For the standard resonator array antenna each $\lambda/2$-patch is separated by a $\lambda/2$-transmission line. This essentially leads to a uniform aperture distribution if all patches are of same width. In terms of a simple circuit model for this antenna, all radiation resistances of same value are parallel. Due to the $\lambda/2$-patch and line length it only provides single-frequency operation.

We use Bloch-Floquet boundaries for the analysis and the design of an antenna array with the patch and the transmission line forming a unit cell. Two resonant modes have been identified with an identical cosine voltage envelop distribution at the patch edges for two different frequencies. One operating frequency is higher $f_+ > f_0$, the other lower $f_- < f_0$ than the $\lambda/2$-frequency f_0. In order for these two frequencies to radiate broadside, it is required that the ends of the overall array are shorted. Due to the dispersion characteristics of the unit cell, positive and negative phase shifts of same magnitude allow a dual-frequency design.

This paper is structured in the following manner, first we propose a simple TL model for the analysis and the design. Based on this model the the resonance frequencies and the corresponding voltage distributions will be derived, using dispersion analysis. Next, we present an antenna concept for a single-frequency antenna with a smooth cosine distribution, which extends our previous work [3] by detailed TL calculation, taking into account all voltages at impedance discontinuities (the patch edges). This is followed by the dual-frequency antenna design procedure along with a parametric study pointing out some limitations. Finally, EM simulation results of a 10 element series-fed patch array antenna are given and compared to the TL model. It is shown that the simple TL model is sufficient to understand and explain the antenna concept.

II. Transmission Line Model and Dispersion

In Fig. 1 the simple TL model composed of two cascaded ideal TL is depicted. A low impedance transmission line is used to model the patch element and high impedance transmission line is used for the connection section, respectively. Since the resonant modes and their distributions are mainly dominated by the reactive components, no radiation loss is taken into account at this stage. Here, the main focus lies on the general concept, keeping the formulas as compact as possible. If we had accounted for moderate radiation loss, the phase of the voltages sampled along the antenna would not have been constant anymore, while the resonant frequencies would have still been the same. For very high radiation loss the resonance distributions and also the resonance frequencies would have been changed and could not have been predicted using this simplified model.

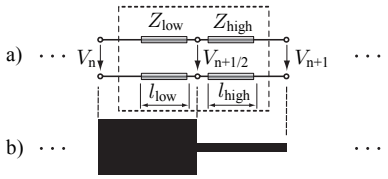

Fig. 1. a) ideal transmission line model for the b) microstrip layout of a low impedance patch and a high impedance connection line.

We use periodic boundaries [4] to derive the dispersion characteristics. The frequency dependent phase shift per unit cell $\Im(\gamma_{\text{cell}}d) = \beta_{\text{cell}}d = \Delta\Phi$ with $d = l_{\text{low}} + l_{\text{high}}$ is calculated as

$$\cos(\Delta\Phi) = \cos(\beta_{\text{low}} l_{\text{low}})\cos(\beta_{\text{high}} l_{\text{high}}) - \frac{1}{2}\frac{Z_{\text{low}}^2 + Z_{\text{high}}^2}{Z_{\text{low}} Z_{\text{high}}}\sin(\beta_{\text{low}} l_{\text{low}})\sin(\beta_{\text{high}} l_{\text{high}}), \quad (1)$$

with the propagation constants β_{low} and β_{high} for the ideal TL sections. The complex propagation constant is know as γ_{cell}, whereas β_{cell} is the phase constant and a real number. In [5] a comprehensive derivation of the dispersion of two cascaded

TLs is given in the context of electromagnetic band gap (EBG) structures.

If the phase variation $\Delta\Phi$ of the unit cell can be adjusted, the overall line can be designed to support a certain global phase shift. When the line ends are terminated with a short circuit, a global resonance distribution can be obtained where the voltages $|V_n|$ follow a spatially sinusoidal envelope distribution. For the design of a N-cell global half-wavelength standing wave sampled at the positions n, the total phase shift has to be

$$N\Delta\Phi = \pm\pi. \tag{2}$$

The required phase shift $\Delta\Phi$ for the proposed $N = 10$ cell antenna is therefore $\Delta\Phi = \pm 18°$ as indicated in Fig. 2.

In Fig. 3 we visualize the key idea of the proposed dual band antenna concept. Two standing wave distributions are sampled at equidistant points. These two spatial distributions exactly differ in λ, one full wavelength. For the lower frequency to total phase shift of each cell accumulates to $-\pi$, while for the higher frequency the total phase accumulates to $+\pi$. Both envelope functions are cosine distributed and of same magnitude. With our patch discontinuities (patch edges) at exactly these positions, we are able to exploit this distribution as radiation aperture.

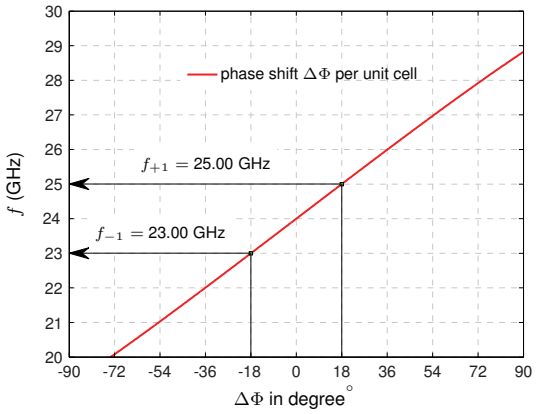

Fig. 2. Dispersion diagram: relates the phase shift of the unit cell to the corresponding frequency. The same $|\Delta\Phi|$ are possible at two different frequencies.

Generally, a certain duality of such two modes can be observed, in a way that modes are corresponding to each other with the same phase shift $|\pm\Delta\Phi|$ at two different frequencies. This duality was already exploited in the context of Composite Right/Left-Handed (CRLH) TLs [3], with the difference that the CRLH-TL unit cell length is much smaller than the fundamentally guided wavelength $d \ll \lambda_g$.

III. Single-Frequency Design

In [6] a single band series fed patch array antenna was proposed with the unique feature of a cosine aperture distribution while using unit cell elements with constant patch widths. Here, we want to show that a smooth cosine function is possible, hence taking into account the inter cell-voltage (other

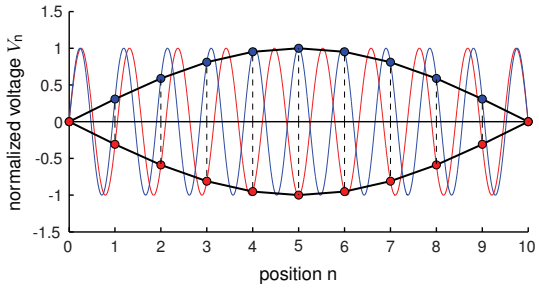

Fig. 3. The normalized voltage distribution for the two frequencies f_- and f_+ shows the equivalent cosine envelop function. In signal processing aliasing frequencies occur for signals sampled at a lower than the Nyquist rate. Here we make use of a spatial aliasing, which is known in the context of image processing, e.g Moiré pattern.

patch edge) $V_{n+1/2}$. By forcing the inter cell voltage to follow the global cosine standing envelope resonant distribution the following formula has been derived:

$$Z_{\text{low}} \sin(\beta_{\text{low}} l_{\text{low}}) = Z_{\text{high}} \sin(\beta_{\text{high}} l_{\text{high}}), \tag{3}$$

which can be used together with (1) to find the electrical line length for the low and high impedance lines. In Fig. 4 equation (1) is plotted for $\Delta\Phi = \pm 18°$ along with equation (3) for a fixed frequency with the two electrical lengths $\beta_{\text{low}} l_{\text{low}}$ and $\beta_{\text{high}} l_{\text{high}}$ varied. The impedance ratio for this setup is $Z_{\text{high}}/Z_{\text{low}} = 3.456$. There are two intersection points, each defining a pair of lengths with a smooth cosine function even for the inter-cell voltage. As a result, there are two different configurations for this antenna type, one configuration has both lines shorter the $\lambda/2$, the other configuration comes with both lines longer than the conventional $\lambda/2$-mode. A circuit model has been setup in ADS with $N = 10$ cascaded unit cells. The first $n = 0$ and the last sampling position $n = 10$ are grounded. The sampled voltages are normalized to the voltage at $n = 5$. Both configurations of Fig. 4, show an identical envelope voltage distribution, Fig. 5.

IV. Dual-Frequency Design

For the dual-frequency design the two resonant frequencies f_- and f_+ have to be specified. The actual length (number of cascaded cells N) and the ratio of the line impedances $Z_{\text{high}}/Z_{\text{low}}$ can be determined. After fixing one of these two parameters, N or $Z_{\text{high}}/Z_{\text{low}}$, the other is dependent. Here, we also use the simple transmission line model depicted in Fig. 1, just to show the parameter dependency as well as the achievable frequency ratios $r = f_+/f_-$. For a proper dual-frequency design it is essential to use a *balanced* unit cell. In CRLH-TL terminology [7] this means that the equivalent series resonator as well as the series resonator have the same resonance frequency. For our cascaded TL structure this simply translates to the electrical line lengths of the low and high impedance lines to be the same. Consequently, the transmission band gap closes and the electrical properties, including the Bloch impedance and the losses, are fully equivalent f_- and f_+. The transition frequency f_0 corresponds to an electrical line length

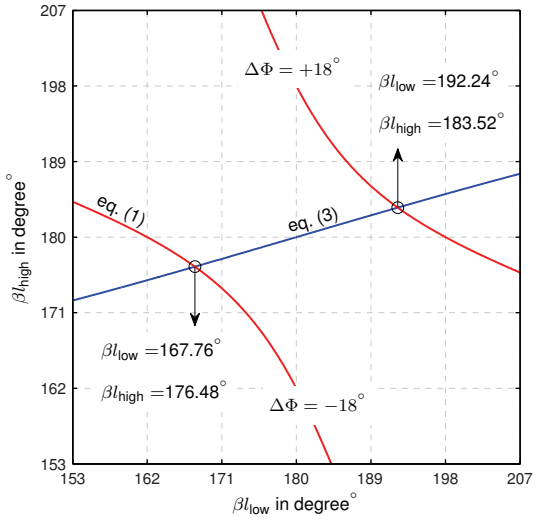

Fig. 4. Single-Frequency Design: Variation of both line lengths at a fixed frequency. Two configurations are possible for a smooth cosine envelop distribution with even the inter-cell voltages following the cosine distribution.

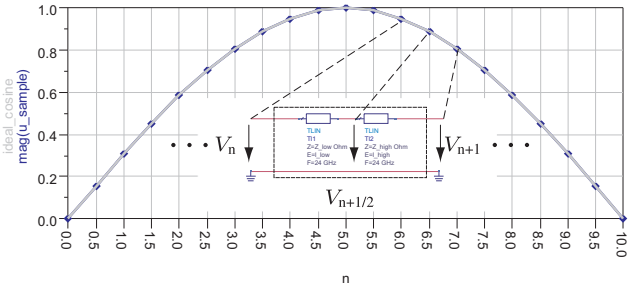

Fig. 5. Single-Frequency Design: ADS circuit simulation of a 10 cell structure with the first and last cell shorted. For both configurations the identical cosine voltage distribution is observed.

of π for both cascaded lines. If we now equate (1), assuming $\beta_{\text{low}} l_{\text{low}} = \beta_{\text{high}} l_{\text{high}} = \beta l$, we find the condition:

$$\cos^2\left(\frac{\pi}{f_0} f_+\right) = \cos^2\left(\frac{\pi}{f_0} f_-\right), \tag{4}$$

with f_0, the frequency where both lines have the electrical length $\beta l = \pi$.

Solving (4) shows that the transition frequency f_0 is simply the arithmetic mean of the two antenna's operating frequencies f_- and f_+.

$$f_0 = \frac{f_+ + f_-}{2} \tag{5}$$

The two remaining design parameters N and the impedance ratio $Z_{\text{high}}/Z_{\text{low}}$ are related as follows. With (1), (2) and (5), the following equation is obtained:

$$\cos\left(\frac{\pi}{N}\right) = \cos^2\left(\frac{\pi}{f_0} f_{+,-}\right)(Z+1) - Z \tag{6}$$

$$\text{with} \quad Z = \frac{1}{2}\frac{Z_{\text{high}}^2 + Z_{\text{low}}^2}{Z_{\text{high}} Z_{\text{low}}} \tag{7}$$

For $f_{+,-}$ either f_+ or f_- can be taken, since f_0 was calculated for the $\cos^2$ to have the same value. Now, equation (6) and (7) can be rearranged so to compute the impedance ratio for a given frequency ratio r and a given length N:

$$Z = \frac{\cos^2\left(\frac{2\pi}{r+1}\right) - \cos\left(\frac{\pi}{N}\right)}{\sin^2\left(\frac{2\pi}{r+1}\right)} \tag{8}$$

$$\frac{Z_{\text{high}}}{Z_{\text{low}}} = \sqrt{Z^2 - 1} + Z \tag{9}$$

In Fig. 6 the parameter dependencies and the achievable frequency ratios are plotted based on the derived formulas (8)-(9). Fig. 6 clearly shows that the length of the overall antenna is the dominant parameter for the design, where as the impedance ratio plays a minor role, especially for a higher number of cascaded cells.

For validation of this design approach we use the circuit simulator in Agilent's ADS to setup a $N = 10$ cell structure with ideal transmission lines. The parameter for this design are: $f_- = 23$ GHz, $f_+ = 25$ GHz, and the calculated impedance ratio $Z_{\text{high}}/Z_{\text{low}} = 3.456$, as indicated in Fig. 6. In Fig. 7 the normalized monitored voltages along the cell position n are plotted for the two frequencies $f_- = 23$ GHz and $f_+ = 25$ GHz. Both curves are identical and the voltage at the integer cell position (cell terminals n) follow exactly the ideal cosine envelop (grey curve). The inter-cell voltages $V_{\text{n+1/2}}$ are sightly off the ideal cosine function compared to the single-frequency design (Fig. 5).

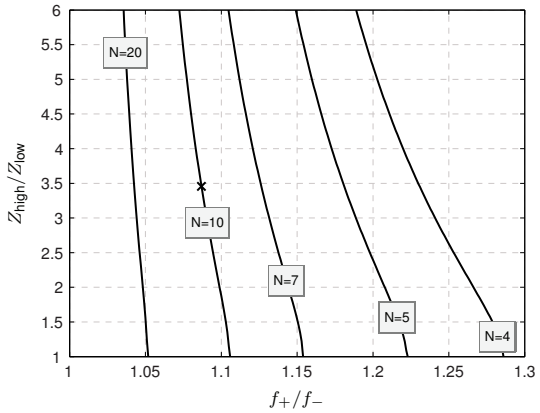

Fig. 6. Dual-Frequency Design: Parameter relation for the dual-frequency design. The marker is placed for $N = 10$ cells and a frequency ratio $r = 25$ GHz/23 GHz $= 1.087$, and the computed impedance ratio $Z_{\text{high}}/Z_{\text{low}}$=3.456.

V. EM Optimization: Unit Cell

In Fig. 8 the microstrip model of the unit cell in the full-wave simulator Empire XCcel is depicted. Unlike the unit cell in the ideal TL model, here, we consider a symmetric unit cell. For a unit cell of an infinite periodic structure the dispersion characteristic $\beta_{\text{cell}} d$ is not affected by a simultaneous shift of both port terminal planes within the unit cell. Evaluating

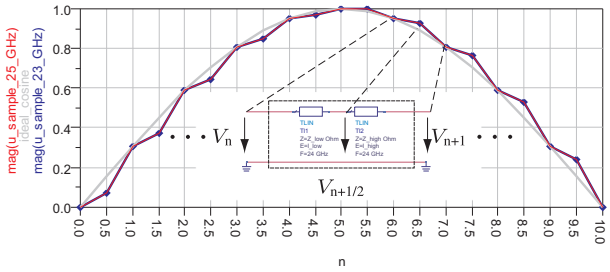

Fig. 7. Dual-Frequency Design: ADS circuit simulation of a 10 cell structure with the first and last cell shorted. For both frequencies the identical cosine voltage distribution is observed. Here, inter-cell voltages $|V_{n+1/2}|$ are not exactly following the cosine distribution

Bloch-Floquet boundary condition for a symmetric cell composed of ideal transmission lines ($\lambda/4$-line, $\lambda/2$-patch, $\lambda/4$-line) will give us the same result as in (1). For the EM unit cell we prefer the terminals at the center of high impedance line, because of better TEM condition. Based on the simulated two port parameters, e.g. admittance parameters, we can directly compute the dispersion of the unit cell. The non-ideal behavior of the microstrip impedance step as well as the radiation is therefore taken into account in the EM cell optimization. For

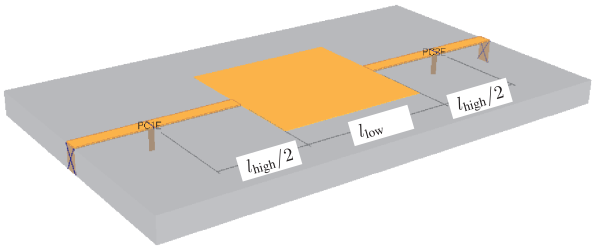

Fig. 8. Dual-Frequency Design: EM model of the symmetric unit cell in Empire XCcel.

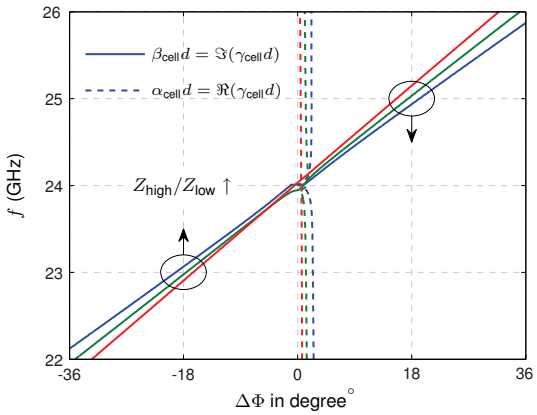

Fig. 9. EM simulation results: Dispersion characteristic for different patch widths, $w_1 = 1575$ μm, $w_2 = 2075$ μm and $w_2 = 3075$ μm. With a variation of the impedance ratio Z_{high}/Z_{low} the frequency ratio r slightly changes. Both line lengths l_{low} and l_{high} had to be re-optimized for each width w.

three different patch widths $w_1 = 1575$ μm, $w_2 = 2075$ μm and $w_2 = 3075$ μm, the unit cell has been optimized (l_{low} and l_{high}) to have a transition frequency $f_0 = 24$ GHz. In Fig. 9 the dispersion of the unit cell for the three patch widths w_1, w_2 and w_3 is shown. It can be seen that with increasing the patch width w the frequency ratio r goes down, as expected from Fig. 6. The frequency ratio is relatively insensitive over changes of the impedance ratio. The main parameter to tune the frequency ratio remains N. One drawback is that the antenna gain also depends on N, so that for this antenna concept these two parameters are no more independent.

VI. Dual-Frequency Series-Fed Patch Array Antenna

Fig. 10 shows the antenna layout with the low impedance patches of length $l_{low} = \lambda/2$ and the high impedance interconnection lines of length $l_{high} = \lambda/2$ at $f_0 = 24$ GHz. The unit cell of width $w_2 = 2075$ μm was chosen to compose the overall antenna. The outer cells are not symmetric and terminated with a via short. We simulated the antenna with

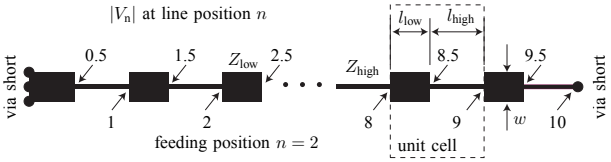

Fig. 10. Microstrip antenna layout: 10 cascaded unit cells with via shorts at the array's ends and voltage monitoring from metalization to ground at the line positions $n \in \{0, 0.5, 1, 1.5, 2, 2.5, .., 10\}$.

the parameters of Rogers RO4003C of 0.5 mm thickness. The qualitative results demonstrating the general duality for the two modes are depicted in Fig. 11. In Fig. 12 quantitative simulation results for the farfield in the xz-plane are plotted along with the voltage distribution monitored at the patches (patch edge to ground). The main lobe and the first side lobe are in good agreement for the two frequencies. The side lobe level suppression above 20 dB also suggests a cosine-distributed near field.

The ideal TL model of the unit cell was modified, so to take into account radiation loss, Fig. 13. The parameters for the lossy TL-model have been obtained by matching the input impedance (circuit simulation data) of the overall antenna to the input impedance (EM simulation results) of the overall antenna. The dispersion characteristics of the lossy TL model and the EM cell are shown in Fig. 14. The unit cell dispersion curves accurately predict the antenna's resonance frequencies. The input impedance of the overall antenna is plotted in Fig. 15. It can been seen the impedance for both resonances f_- and f_+ are equivalent in terms of bandwidth and losses. The good agreement is due to the mapping to the actual EM results. Nevertheless, this shows that the chosen lossy TL model sufficiently supports the proposed concept.

The feeding is done by a probe feeding at line position $n = 2$. The matching is adjusted by simply moving this feed probe along the sampling points n. The minimum input impedance is found at the outer short of the array

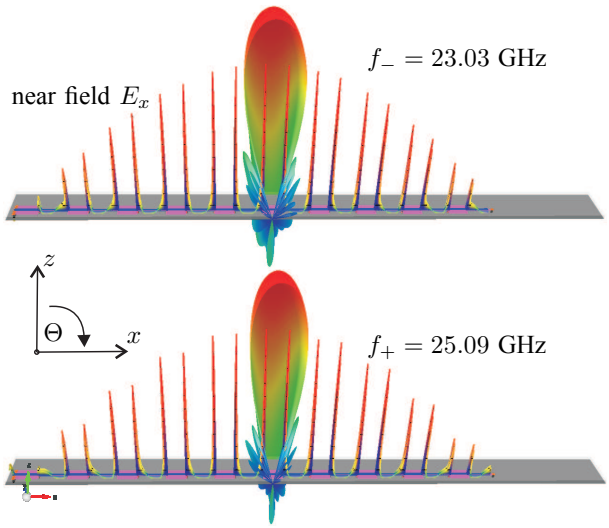

Fig. 11. EM simulation model in Empire XCcel: 3D farfield and the near field component E_x in the metalization layer is shown. The E_x field component at the patch edges corresponds to the voltages $|V_\mathrm{n}| \propto |E_{z,\mathrm{n}}|$, due to the stray field at the edges.

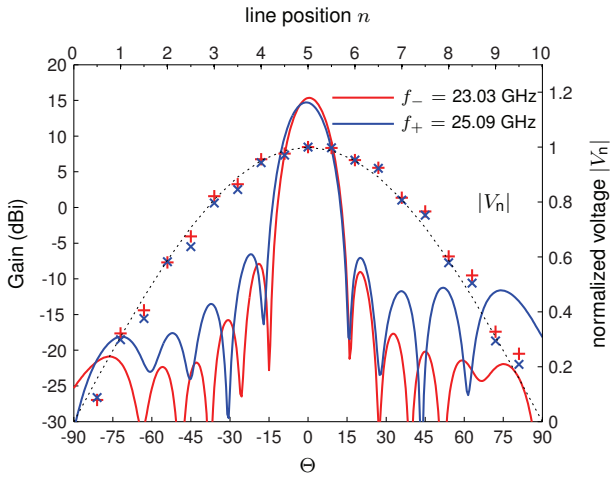

Fig. 12. Farfield ($\varphi = 0$) and voltage distribution normalized to the array center position $n = 5$.

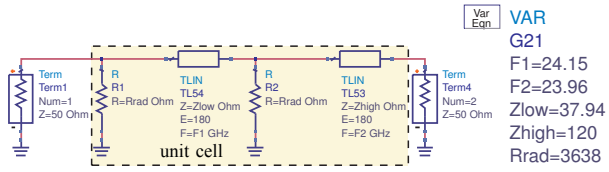

Fig. 13. Extended TL model with resistor R to take into account the radiation loss.

($n = 0$ or $n = 10$) and increases, if we move the feed to the center position $n = 5$.

VII. Conclusions

We presented a novel antenna concept, which simply employs the well known microstrip patch array with the array ends shorted. The conventional uniform distribution is not supported anymore, but two cosine distributed modes at a lower and higher frequency having broadside radiation with a low side lobe level.

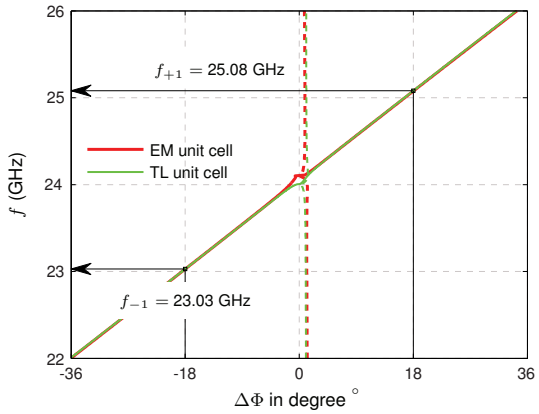

Fig. 14. Comparison of the EM-simulated unit cell with the TL unit cell.

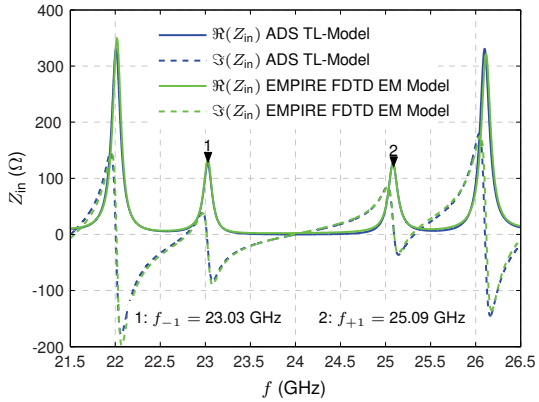

Fig. 15. Input impedance of the overall antenna fed at line position $n = 2$. The EM-model and the TL-model agree well. The resonance characteristic and the impedance bandwidth for f_- and f_+ are equivalent due to the identical field distribution.

References

[1] W. Menzel, "A 40 ghz microstrip array antenna," in *Proc. MTT-S International Microwave Symposium Digest*, vol. 80, no. 1, 1980, pp. 225–226.

[2] T. Metzler, "Microstrip series arrays," *IEEE Trans. Antennas Propagat.*, vol. 29, no. 1, pp. 174–178, 1981.

[3] S. Otto, A. Rennings, C. Caloz, P. Waldow, and T. Itoh, "Composite right/left-handed λ-resonator ring antenna for dual-frequency operation," in *Proc. IEEE Antennas and Propagation Society International Symposium*, July 2005, pp. 684–687.

[4] D. M. Pozar, *Microwave Engineering*. J.Wiley & Sons, New York, 2nd ed., 1998.

[5] A. Foroozesh and L. Shafai, "Wave propagation in 1d ebgs: Periodic multilayer films consisting of two different materials," *IEEE Antennas Propagat. Mag.*, vol. 50, no. 2, pp. 175–182, 2008.

[6] S. Otto, O. Litschke, J. Leiß, and K. Solbach, "A unit cell based low side lobe level design for series-fed array," in *Proc. Asia-Pacific Microwave Conference (APMC), Hong Kong, Dec. 2008, CD-ROM*, 2008.

[7] C. Caloz and T. Itoh, *Electromagnetic Metamaterials: Transmission Line Theory and Microwave Applications*. Wiley-IEEE Press, 2005.